PSI Injector II and the 72 MeV transfer line: MinT-Simulation vs. Measurements

PAUL SCHERRER INSTITUT

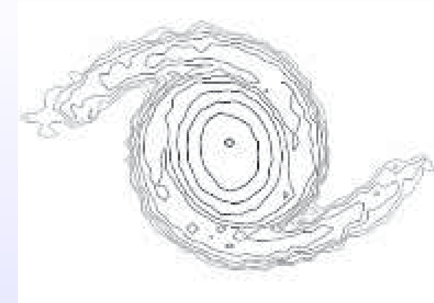

C. Baumgarten and H. Zhang

Paul Scherrer Institut, 5232 Villigen-PSI, Switzerland

Abstract

PSI's Injector II cyclotron is the only cyclotron worldwide that makes use of the so-called "Vortex effect", in which the space charge force leads to the counter-intuitive effect to "roll up" bunches, thus keeping them longitudinally compact. The effect has been confirmed by bunch shape measurements and the PIC-simulations with OPAL. However, PSI's new fast matrix code MinT allows to reproduce the Vortex effect by a linear matrix model which is computational much cheaper than PIC simulations, and is suitable for "online use" in Control rooms. Furthermore it provides the second moments σ_{ij} of matched distributions. We compare results of various measurements with MinT calculations which show that the linear model works well and provides excellent initial conditions to fit the beam profiles of the 72 MeV transfer line to the Ring cyclotron.

PSI's High Intensity Proton Accelerator (HIPA)

Figure 1 shows PSI's High Intensity Proton Accelerator (HIPA) [1]: A Cockcroft-Walton DC pre-accelerator provides a 870 keV proton beam of typically 10 mA DC current. Two (first and third harmonic) bunchers are used to generate 50 MHz CW bunch structure before the beam is axially injected into the first turn of Injector II. The beam is extracted at 72 MeV from Injector II and transported with the IW2-beamline towards the PSI's Ring cyclotron. The 590 MeV beam is used to generate pions and muons at two graphite targets and for neutron production in the Swiss spallation source SINQ (not shown).

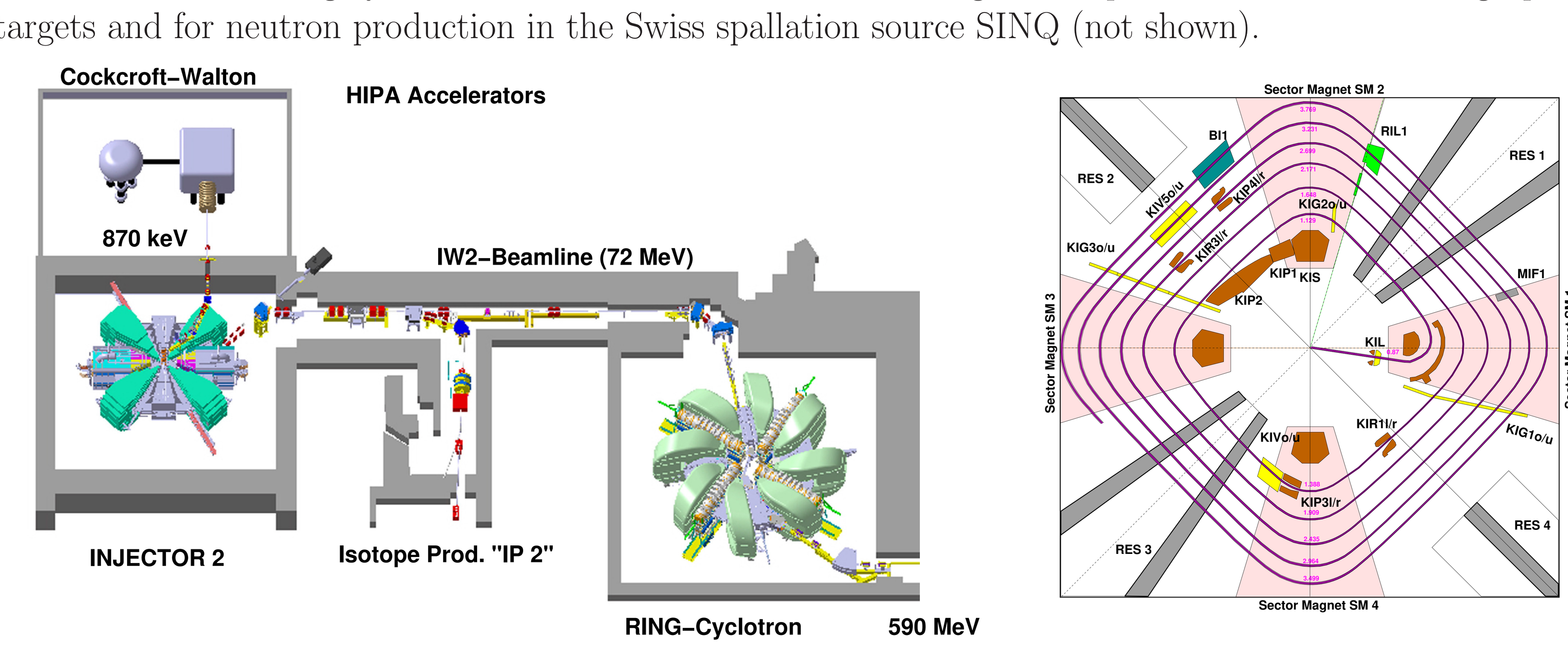

FIGURE 1: Left: Overview of PSI's High Intensity Proton Accelerators (HIPA). Right: The central region of Injector II with various collimators.

The Vortex Effect

The Vortex effect [2] (or "negative mass instability" [3]) is due to strong space charge of bunches in the isochronous regime of circular accelerators. The space charge force induces coupling terms between the longitudinal and the transverse-horizontal beam motion [4, 5]. This coupling leads to almost round bunches with dense and matched cores and halos with (typically) two tails [6, 7]. In the core of the bunch, the space charge force is approximately linear and the linear matching conditions can be computed, if beam current and core emittances are known [5, 8, 9]. The first turns of Injector II are equipped with several sets of adjustable collimators, which allow to remove the halo and extract the beam with low losses, if the orientation of the halo tails at the collimator is transverse [10]. The relative orientation of the tails depend on the details of the bunch formation and the strength of the space charge force. If the halo orientation depends on the bunch charge, then this leads to a non-linear current dependency of the losses, possibly as shown in Fig. 2.

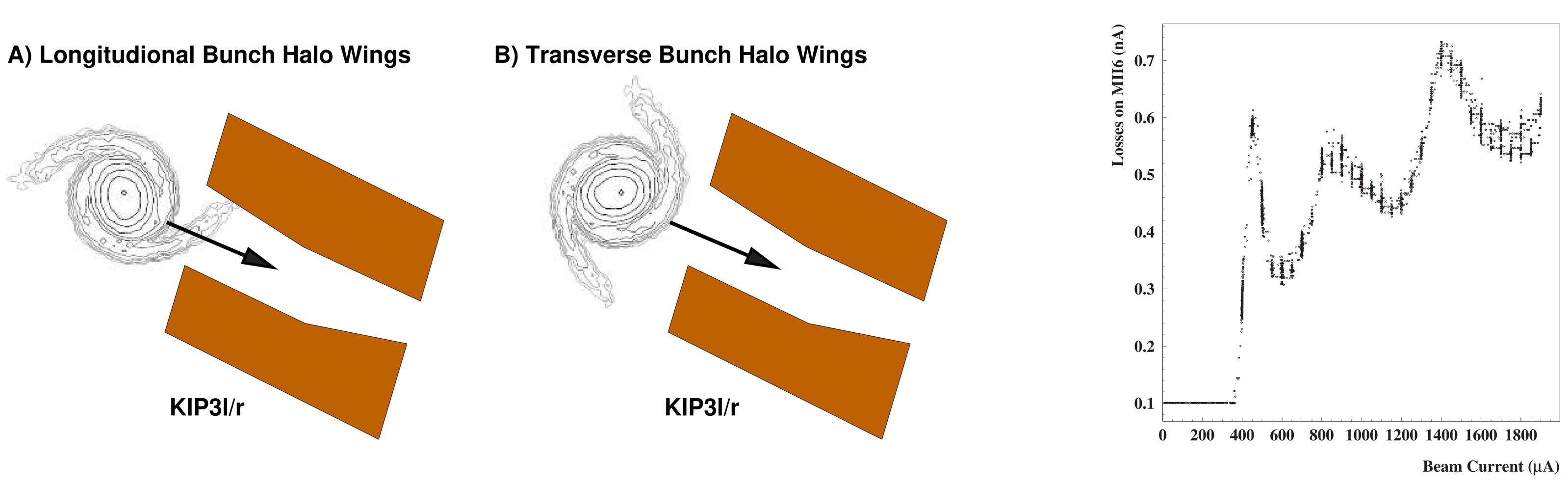

FIGURE 2: Left: Removal of halo tails depends on orientation. Right: Beam losses vs. beam current measured by ionization chamber MII6, located behind the electrostatic extractor "EID" of Injector II.

The IW2 Beamline

PSI's new fast beam optics code MinT (**M**in**T** **i**s **n**ot **T**ransport) [11] enables to compute the matched beam parameters for arbitrary symplectic transfer matrices for given current and emittance(s). These matched beam conditions, evaluated for the last turn of Injector II, allow for an accurate prediction of the beam envelope in the IW2 beamline based on only three parameters, namely beam current and two emittances.

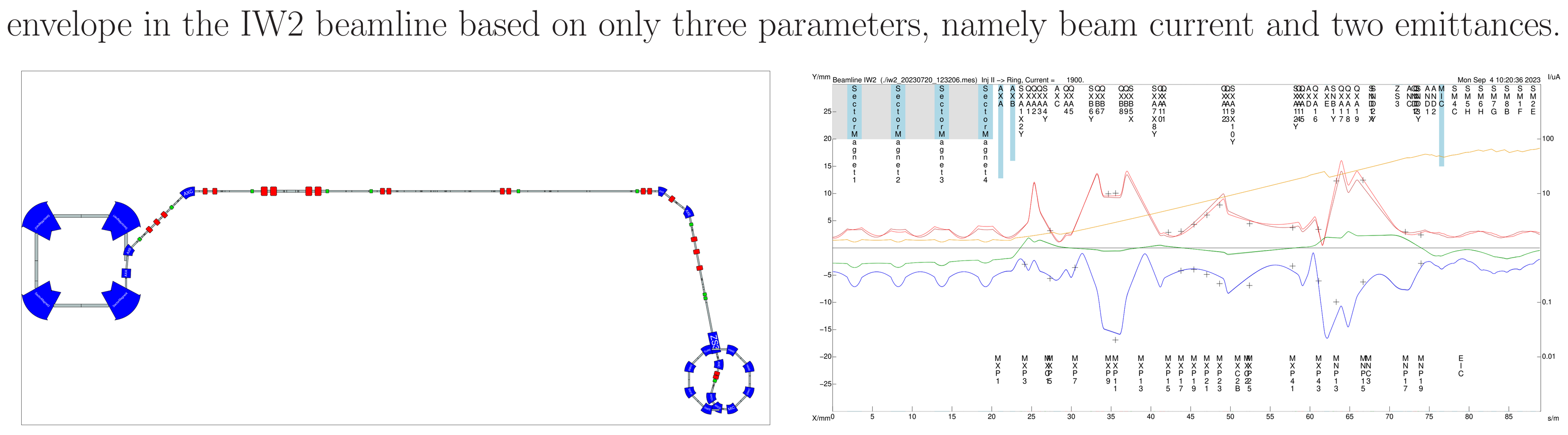

FIGURE 3: Left: Layout of the IW2 beamline, from the last turn of Injector II to the first turn of the Ring cyclotron. Right: TRANSPORT style plot of beam envelopes, i.e. $-2\,\sigma_x$ (blue), $2\,\sigma_y$ (red) and $\sigma_z/2$ (orange), in the IW2 beamline, assuming a matched beam (dark colors) and - in lighter colors - a horizontally matched beam with the vertical beam parameters matched to reproduce the measured beam sizes (cross markers).

Beam Emittance vs. Current

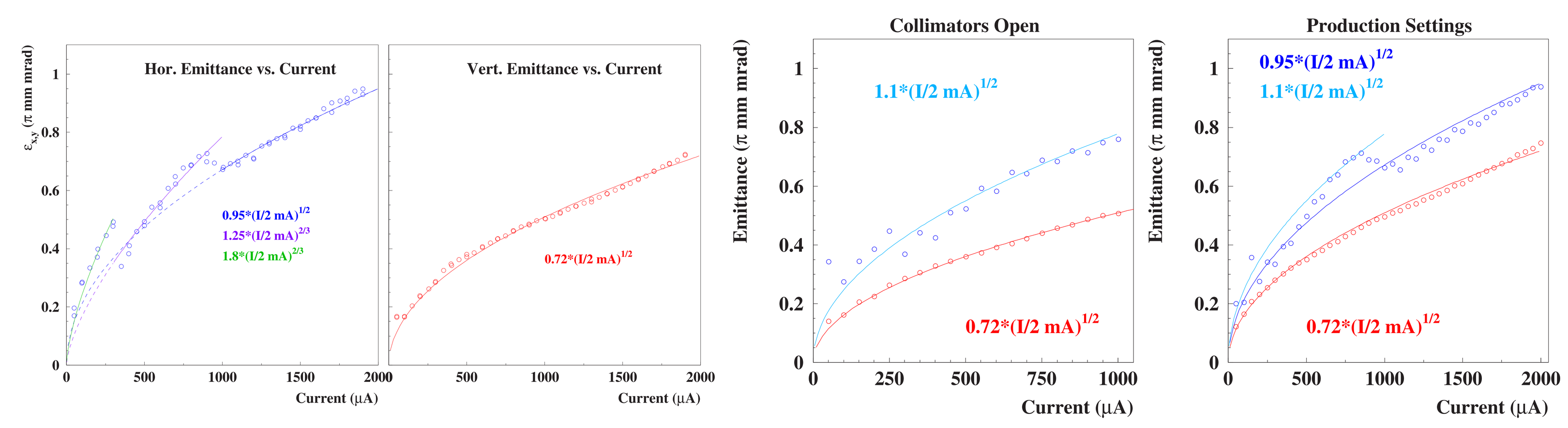

FIGURE 4: Left two plots: Horizontal and vertical eigen-emittance vs. current (circles) from MinT-fits for production settings, measured 2023-07-20. Right two plots: Same measurements (circles) for two different collimator settings, namely "open" and "production", measured 2023-08-04. The plotted functions are not fitted, but only "guides for the eyes".

We measured the beam profiles of the IW2-beamline for various beam currents (controlled by the position of collimator KIP2) and fitted the horizontal beam envelope with one free parameter, namely the transverse horizontal emittance eigenvalue. In a second step, the vertical beam parameters $(\sigma_{33}, \sigma_{34}, \sigma_{44})$ were varied to improve the matching of the vertical beam envelope. The emittances are plotted versus beam current in Figs. 4. Besides the local emittance maximum below 1 mA, presumably caused by beam halo, the emittance obeys a law of proportionality

$$\varepsilon/\varepsilon_0 = \sqrt{I/I_0}\,. \tag{1}$$

Measurements with the Radial Probe RIE2

Besides the beam profile monitors, we used the (short) radial probe "RIE2", which is located at the sector edge shortly before the septum magnet.

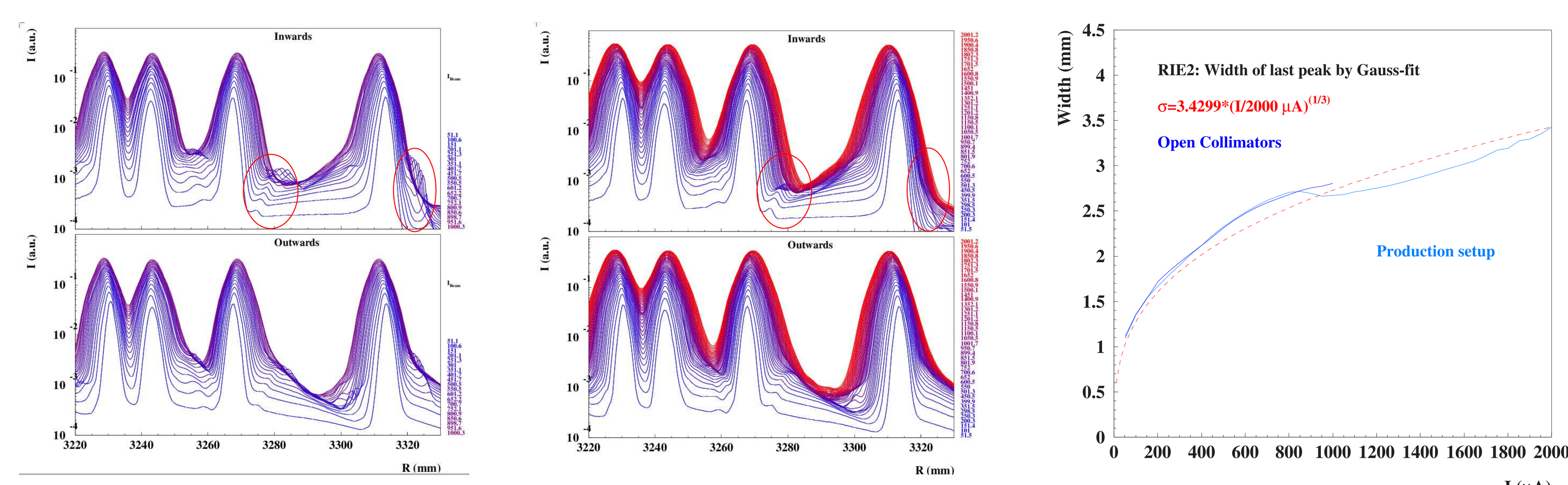

FIGURE 5: Left: RIE2-scans (inwards and outwards) for "open collimators". Center: RIE2-scans (inwards and outwards) for "production settings". (In both plots the location of potential traces of beam halo are marked by red ellipses.) Right: Width of the last peak of the RIE2 scan vs. beam current.

As a closer look on Fig. 5 reveals, the last RIE2 peak of the production setup has no "satellite" as the one for collimator open. The satellite peak is likely a remainder of a beam halo tail, which is cut in case of production collimators. Theoretical considerations for spherical bunches ($\sigma \approx \sigma_x \approx \sigma_y \approx \sigma_z\,\gamma$) allow to derive the approximation [5]:

$$\sigma^4 - C_0\,I\,\sigma - C_1\,\varepsilon^2 = 0 \tag{2}$$

with two constants C_0 and C_1. Inserting $I = C_2\,\varepsilon^2$ then results in

$$\varepsilon = \frac{\sigma^2}{\sqrt{C_0\,C_2\,\sigma + C_1}} \quad \text{and} \quad \mathrm{I} = \frac{\sigma^4}{\mathrm{C}_0\,\sigma + \mathrm{C}_1/\mathrm{C}_2}\,. \tag{3}$$

In the case of emittance (space charge) domination one therefore expects $\sigma \propto I^{1/4}$ ($\sigma \propto I^{1/3}$).

Summary and Conclusion

OPAL-simulations [12] of Injector II and the IW2-beamline have been done before [10, 13]. But PIC-simulations are not required to reproduce the beam envelopes, if it is known that the beam is matched – as in case of Injector II. The linear matching model of MinT provides sufficient information to compute the starting conditions for the calculation of the second moments of the IW2-profiles.
The current dependence and the measured losses indicate that the beam halo is effectively removed at production current, though parts of the beam halo seem to survive up to extraction at intermediate currents. The results are an important step towards a more detailled and comprehensive understanding of the bunch formation in Injector II.

References

[1] J. Grillenberger, C. Baumgarten, and M. Seidel. The High Intensity Proton Accelerator Facility. *SciPost Phys. Proc.*, 5(2), 2021.

[2] M. M. Gordon. The longitudinal space charge effect and energy resolution. In R.W. McIlroy, editor, *5th International Cyclotron Conference*, pages 305–317. Butterworth London (1971), September 1969.

[3] C. E. Nielsen, A.M. Sessler, and K.R. Symon. Longitudinal instabilities in intense relativistic beams. In L. Kowarski, editor, *Proceedings of the 2nd International Conference on High-Energy Accelerators and Instrumentation (HEACC 1959)*, pages 239–252, Geneva, September 14-19 1959. CERN.

[4] P. Bertrand and Ch. Ricaud. Specific cyclotron correlations under space charge effects in the case of a spherical beam. In F. Marti, editor, *Proceedings of the 16th International Conference on Cyclotrons and their Applications*, pages 379–382. American Institute of Physics (2001), may 13-17 2001.

[5] C. Baumgarten. Transverse-longitudinal coupling by space charge in cyclotrons. *Phys. Rev. ST Accel. Beams*, 14.

[6] R. Koscielniak and S. Adam. Simulation of space-charge dominated beam dynamics in an isochronous avf cyclotron. In Steven T. Corneliussen and Linda Carlton, editors, *Proceedings of the 1993 Particle Accelerator Conference (PAC 93)*, pages 3639–3641, Piscataway, NJ, May 17-20 1993. IEEE.

[7] S. Adam. Space charge effect in cyclotrons - from simulations to insights. In J. Comell, editor, *Proceedings of the 14th International Conference on Cyclotrons and their Applications*, pages 446–448. World Scientific, oct 1995.

[8] C. Baumgarten. A Geometrical Method of Decoupling. *Phys. Rev. ST Accel. Beams*, 15:124001, 2012.

[9] C. Baumgarten. Transverse-longitudinal coupling by space charge in cyclotrons. In Jana Thomson and Volker Schaa, editors, *Proceedings of the 20th International Conference on Cyclotrons and their Applications*, pages 316–319. JaCoW, jul 2013.

[10] A. Kolano, A. Adelmann, R. Barlow, and C. Baumgarten. Intensity limits of the PSI Injector II cyclotron. *Nuclear Instruments and Methods in Physics Research Section A: Accelerators, Spectrometers, Detectors and Associated Equipment*, 885:54–59, 2018.

[11] C. Baumgarten. MinT: A Fast Lightweight Envelope/Monte-Carlo Beam Optics Code for the Proton Beamlines of the Paul Scherrer Institute. *arXiv.org:2202.07245*, 2022.

[12] Andreas Adelmann, Pedro Calvo, Matthias Frey, Achim Gsell, Uldis Locans, Christof Metzger-Kraus, Nicole Neveu, Chris Rogers, Steve Russell, Suzanne Sheehy, Jochem Snuverink, and Daniel Winklehner. OPAL a Versatile Tool for Charged Particle Accelerator Simulations. *arxiv:1905.06654*, 2019.

[13] Y. J. Bi, A. Adelmann, R. Dölling, M. Humbel, W. Joho, M. Seidel, and T. J. Zhang. Towards quantitative simulations of high power proton cyclotrons. *Phys. Rev. ST Accel. Beams*, 14:054402, May 2011.